# High-Temperature, Single-Crystal X-ray Study of Natrolite[1]

Donald R. Peacor

*Department of Geology and Mineralogy, The University of Michigan,
Ann Arbor, Michigan 48104*

## Abstract

Natrolite from Bergen Hill, New Jersey, is shown to dehydrate to metanatrolite at approximately 250°C. Rehydration occurs rapidly even at temperatures as high as 210°C. The crystal structure was refined with data measured at 25°C, 88°C, 146°C and 198°C, with $R$-values of 2.1 to 2.2 percent. $T$–O and O–O distances, as calculated with no thermal correction, reflect apparent slight contraction for the Si tetrahedra but no changes in the Al tetrahedron. The low thermal expansion for the hydrated phase is explained by the negligible changes in atom coordinates as a function of temperature.

## Introduction

The crystal structure of natrolite was originally formulated by Pauling (1930). Atomic positions were subsequently determined by Taylor, Meek, and Jackson (1933); Meier (1960) confirmed and refined the structure, using data measured at room temperature. There is now some interest in not only determining structure parameters at room temperature, but in determining the nature of change in structure as a function of temperature. We have undertaken this study on natrolite, then, for the following reasons. First, by comparison with most other tektosilicates, particularly zeolites, the structure of natrolite is relatively simple. Secondly, natrolite undergoes dehydration at relatively low temperatures. The loss of water occurs in a simple, one-step process. Those structure parameters associated with dehydration, if any, should thus be most readily characterized in natrolite. This work has been carried out in two phases. First, in order to establish the general nature of changes as a function of temperature and with particular reference to dehydration, the changes in intensity and position of a selected set of peaks have been studied as a function of temperature. Secondly, three-dimensional intensity data have been measured, and the structure refined, for four temperatures below that of dehydration.

## Experimental

The specimens used in this study were obtained from The University of Michigan mineralogical collections, and were originally collected at Bergen Hill, New Jersey. Published analyses for natrolite from this and nearby related localities consistently show that the Si:Al ratio is near the ideal of 3:2, and that only minor proportions of K and Ca substitute for Na. It was therefore assumed that the Bergen Hill specimens were very near to the ideal formula $Na_2Al_2Si_3O_{10} \cdot 2H_2O$. The space group was verified as being $Fdd2$, as determined by Meier (1960). Lattice parameters were measured using the Weissenberg-geometry diffractometer and are $a = 18.43$, $b = 18.71$ and $c = 6.52$ Å.

All data was obtained using crystals measuring approximately $0.3 \times 0.3 \times 0.5$ mm, mounted within silica glass capillaries for rotation about the $c$-axis. These were mounted on a Weissenberg-geometry diffractometer fitted with the furnace described by Foit and Peacor (1967) and a scintillation counter. MoK$\alpha$ radiation, monochromated with a flat crystal of graphite, was used. Temperature was measured using a chromel-alumel thermocouple. To study selected reflections as a function of temperature, intensities were graphically recorded and measured with a planimeter. Zero-level two-theta values were measured by determining the midpoint between two positions of equal intensity on the low and high $\theta$ sides of the peaks. Three-dimensional intensity values were determined using the Supper-Pace automated system, which employs measure-

ment of background on two sides of a peak. Data were measured at temperatures of 25, 88, 146, and 198°C. All intensities were corrected for Lorentz and polarization factors (including a monochromator factor) and absorption ($\mu = 7.1$ cm$^{-1}$). Minimum observed intensity values were assigned to weak reflections on the basis of standard counting statistics. The final corrected data sets contained 636 to 638 symmetry-independent structure amplitudes.

Full matrix least-squares refinement was carried out under the following conditions: (1) The weighting scheme of Cruickshank (1965) was used throughout. (2) Form factors were used assuming half-ionization of all atoms. (3) Starting atom parameters were those of Meier (1960). In the final stages of refinement, anisotropic temperature factors were varied, and refinements were completed with cycles in which the scale factor, coordinates and anisotropic temperature factors were allowed to vary. The final *R*-values are 2.1 percent (25°C), 2.1 percent (88°C), 2.2 percent (146°C) and 2.2 percent (198°C). Observed and calculated structure factors are listed in Table 1.[2]

## Selected Peaks as a Function of Temperature

Fang (1963), using single crystal X-ray methods, found that natrolite dehydrates in a single step at 300°C, with decreases in the magnitudes of *a* and *b* of 10.7 and 8.3 percent, respectively, and with no observable change in *c*. Van Reeuwijk (1972) reviewed other studies of the dehydration process. He noted that the dehydration temperatures determined by other investigators using DTA and TGA methods are too high in that they do not represent equilibrium temperatures. Using high-temperature powder X-ray techniques, he verified that the water is lost in a single step, "with an initial temperature of *ca* 240°C," and with the transition at 280°C to metanatrolite, the dehydrated equivalent of natrolite.

The integrated intensity of some selected reflections for the Bergen Hill natrolite (Fig. 1) show a continuous decrease in intensity with increasing temperature. Since some atom positional shifts should cause some intensities to increase, this shows

that atom thermal vibration must be increasing at a significant rate relative to shifts in atom positions in order to cause an overall decrease in intensity.

All intensity measurements were made only after verifying that a steady-state condition had been reached at a given temperature. Up to approximately 220°C, all intensity changes had been immediate with increase in temperature. For temperatures in excess of 220°C, time periods of 5-10 minutes were required for intensities to decrease slightly and come to a steady-state condition. At approximately 245–250°C (variable for different crystals), intensities dropped rapidly to zero. These results confirm that the dehydration occurs increasingly from 220 to 250°C, with the bulk of the water being lost over a very narrow temperature range near 250°C.

Lattice parameters *a* and *b* at about 260°C for the dehydrated phase, metanatrolite, were determined as 17.05 and 16.20 Å, respectively. This is in good agreement with the results of Fang (1963). For the first crystal studied, Weissenberg photographs were taken immediately after cooling to room temperature, subsequent to dehydration. All peaks were broad and diffuse, but retained the relative intensities and positions of the original natrolite.
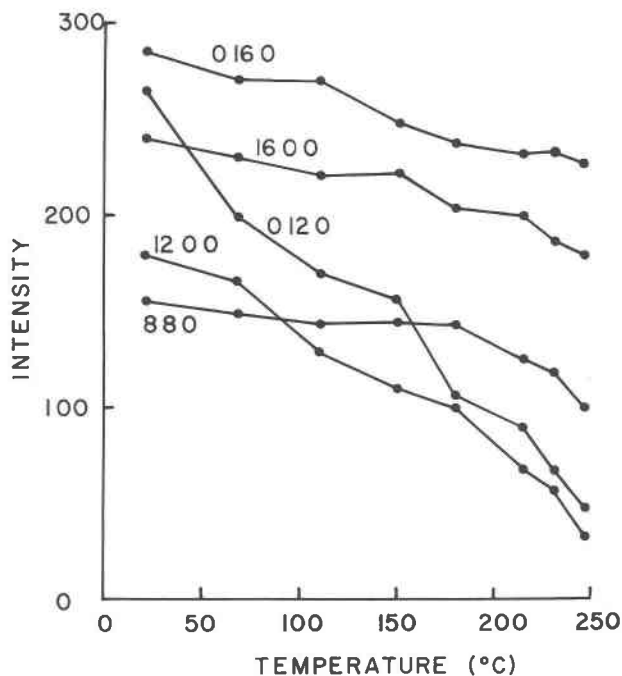


FIG. 1. Intensities of selected reflections of natrolite as a function of temperature. At approximately 250°C, dehydration occurs.

Measurements of $a$ and $b$ showed that they were unchanged. This should be possible only if the natrolite had rehydrated. In subsequent heating experiments it was found that following dehydration to metanatrolite at 250°C, cooling the crystal to about 210°C resulted in rapid rehydration. Reheating caused dehydration to again occur at 250°C. It is thus clear, at least for Bergen Hill natrolite, that room temperature studies in an ordinary atmosphere would always be of the hydrated phase, and not of metanatrolite. Hey and Bannister (1933) noted that specimens dehydrated at 300 to 350°C and examined at room temperature exhibit no changes, and that specimens dehydrated at 400 to 600°C differed optically from natrolite, but that diffraction patterns were unchanged (except that the dehydrated phase gave poor photographs, presumably due to diffuseness of reflections). At higher temperatures, metanatrolite may therefore undergo further change which subsequently acts to prevent rehydration to natrolite during the cooling process.

Meier (1960) noted that, contrary to generally accepted views, dehydration should occur through $H_2O$ loss through intersecting channels between neighboring chains, and thus perpendicular to $c$. He showed that the channels parallel to $c$ are much narrower than those perpendicular to $c$. Our heating experiments provide some evidence for the true mechanism. In one experiment, the temperature was rapidly lowered to room temperature with the dehydration process not having been allowed to go to completion. Since dehydration results in the crystal becoming opaque white, the dehydrated and hydrated sections of the crystal are readily distinguished. The ends of the crystal had been affected but not the center. It therefore seems clear that dehydration must occur with diffusion of $H_2O$ through the channels parallel to $c$.

### Crystal Structure Relations

Table 2 is a compilation of the refined structure parameters for each of the four temperatures at which data was measured. Tables 3–5 contain values of interatomic distances and angles, with standard errors as calculated using the least-squares variance-covariance matrix and lattice parameter standard errors. Several atomic coordinates, especially $x$ and $y$ of Si(2) and Al, appear to show shifts with changing temperature which are uniformly in a single direction. However, the changes are so small relative to the standard errors, especially for the oxygens,

TABLE 2. Coordinates and Equivalent Isotropic Temperature Factors at Different Temperatures*

| Atom | | 25°C | 88°C | 146°C | 198°C |
|---|---|---|---|---|---|
| Si(1) | x | 0 | 0 | 0 | 0 |
| | y | 0 | 0 | 0 | 0 |
| | z | 0.0 | 0.0 | 0.0 | 0.0 |
| | B | 0.52 | 0.63 | 0.75 | 0.82 |
| Si(2) | x | .15327(3) | .15342(3) | .15355(3) | .15361(3) |
| | y | .21139(3) | .21121(3) | .21113(3) | .21116(3) |
| | z | .62286(24) | .62285(23) | .62294(22) | .62266(23) |
| | B | 0.48 | 0.56 | 0.67 | 0.73 |
| Al | x | .03740(3) | .03748(3) | .03769(3) | .03772(4) |
| | y | .09368(3) | .09357(3) | .09333(3) | .09329(3) |
| | z | .61540(26) | .61517(24) | .61589(25) | .61584(25) |
| | B | 0.49 | 0.56 | 0.66 | 0.74 |
| O (1) | x | .0228(1) | .0228(1) | .0230(1) | .0230(1) |
| | y | .0683(1) | .0680(1) | .0679(1) | .0679(1) |
| | z | .8654(5) | .8652(5) | .8657(5) | .8659(5) |
| | B | 1.09 | 1.30 | 1.56 | 1.73 |
| O (2) | x | .0702(1) | .0704(1) | .0707(1) | .0708(1) |
| | y | .1818(1) | .1815(1) | .1812(1) | .1812(1) |
| | z | .6094(4) | .6093(4) | .6091(4) | .6093(5) |
| | B | 0.65 | 0.84 | 0.88 | 1.05 |
| O (3) | x | .0983(1) | .0985(1) | .0984(1) | .0986(1) |
| | y | .0351(1) | .0350(1) | .0349(1) | .0349(1) |
| | z | .5005(5) | .5002(5) | .4996(5) | .5002(5) |
| | B | 1.03 | 1.19 | 1.41 | 1.58 |
| O (4) | x | .2064(1) | .2065(1) | .2068(1) | .2068(1) |
| | y | .1529(1) | .1529(1) | .1530(1) | .1531(1) |
| | z | .7255(5) | .7262(5) | .7259(5) | .7248(5) |
| | B | 1.02 | 1.23 | 1.35 | 1.54 |
| O (5) | x | .1805(1) | .1807(1) | .1810(1) | .1808(1) |
| | y | .2275(1) | .2270(1) | .2270(1) | .2272(1) |
| | z | .3900(5) | .3904(5) | .3910(5) | .3909(5) |
| | B | 1.06 | 1.30 | 1.51 | 1.74 |
| Na | x | .2207(1) | .2208(1) | .2208(1) | .2209(1) |
| | y | .0308(1) | .0308(1) | .0308(1) | .0311(1) |
| | z | .6176(3) | .6174(3) | .6173(4) | .6170(4) |
| | B | 1.34 | 1.67 | 2.02 | 2.38 |
| $H_2O$ | x | .0563(1) | .0567(1) | .0568(1) | .0574(2) |
| | y | .1894(1) | .1893(1) | .1895(1) | .1891(1) |
| | z | .1109(6) | .1107(6) | .1109(7) | .1098(8) |
| | B | 1.81 | 2.15 | 2.59 | 3.16 |

*Estimated standard deviations (esd) as given in parentheses in this and subsequent tables refer to the last decimal place cited. Thus 0.15327(3) and 0.0228(1) indicate esd's of 0.00003 and 0.0001, respectively.

TABLE 3. Cation-Oxygen Distances

| | | 25°C | 88°C | 146°C | 198°C |
|---|---|---|---|---|---|
| Si(1) | –O(1) | 1.606(4) | 1.602(4) | 1.601(4) | 1.599(4) |
| | O(5) | 1.628(4) | 1.629(4) | 1.628(4) | 1.629(4) |
| | ave. | 1.617 | 1.615 | 1.614 | 1.614 |
| Si(2) | –O(2) | 1.631(4) | 1.629(4) | 1.628(4) | 1.629(4) |
| | O(3) | 1.611(4) | 1.611(4) | 1.609(4) | 1.612(4) |
| | O(4) | 1.614(4) | 1.613(3) | 1.611(3) | 1.607(4) |
| | O(5) | 1.627(5) | 1.624(5) | 1.622(5) | 1.621(5) |
| | ave. | 1.621 | 1.619 | 1.618 | 1.617 |
| Al | –O(1) | 1.720(6) | 1.721(6) | 1.719(6) | 1.720(6) |
| | O(2) | 1.756(5) | 1.753(5) | 1.754(5) | 1.754(5) |
| | O(3) | 1.738(4) | 1.740(4) | 1.738(4) | 1.738(4) |
| | O(4) | 1.751(4) | 1.747(4) | 1.749(4) | 1.754(5) |
| | ave. | 1.741 | 1.740 | 1.740 | 1.742 |
| Na | –O(2) | 2.517(5) | 2.521(5) | 2.525(5) | 2.526(6) |
| | O(2)' | 2.613(6) | 2.620(6) | 2.625(6) | 2.627(6) |
| | O(3) | 2.384(6) | 2.381(6) | 2.385(6) | 2.379(6) |
| | O(4) | 2.404(6) | 2.406(6) | 2.407(6) | 2.402(6) |
| | $H_2O$ | 2.367(6) | 2.370(6) | 2.370(6) | 2.380(7) |
| | $H_2O$ | 2.385(6) | 2.387(6) | 2.388(6) | 2.396(7) |
| | ave. | 2.445 | 2.447 | 2.450 | 2.452 |

TABLE 4. O–O Distances for Tetrahedra*

| Tetrahedron | 25°C | 88°C | 146°C | 198°C |
|---|---|---|---|---|
| Si(1) tetrahedron | | | | |
| O(1)-O(1) | 2.690 | 2.678 | 2.679 | 2.678 |
| O(1)-O(5) | 2.613 | 2.610 | 2.609 | 2.610 |
| O(1)-O(5)' | 2.615 | 2.617 | 2.615 | 2.611 |
| O(5)-O(5)' | 2.697 | 2.696 | 2.686 | 2.689 |
| ave. | 2.641 | 2.638 | 2.636 | 2.635 |
| Si(2) tetrahedron | | | | |
| O(2)-O(3) | 2.615 | 2.612 | 2.612 | 2.611 |
| O(2)-O(4) | 2.677 | 2.675 | 2.673 | 2.669 |
| O(2)-O(5) | 2.629 | 2.625 | 2.623 | 2.623 |
| O(3)-O(4) | 2.676 | 2.676 | 2.674 | 2.674 |
| O(3)-O(5) | 2.640 | 2.641 | 2.634 | 2.637 |
| O(4)-O(5) | 2.639 | 2.636 | 2.629 | 2.626 |
| ave. | 2.646 | 2.644 | 2.641 | 2.640 |
| Al tetrahedron | | | | |
| O(1)-O(2) | 2.839 | 2.840 | 2.840 | 2.840 |
| O(1)-O(3) | 2.826 | 2.827 | 2.830 | 2.831 |
| O(1)-O(4) | 2.873 | 2.868 | 2.872 | 2.879 |
| O(2)-O(3) | 2.882 | 2.878 | 2.874 | 2.874 |
| O(2)-O(4) | 2.769 | 2.766 | 2.765 | 2.769 |
| O(3)-O(4) | 2.865 | 2.868 | 2.859 | 2.865 |
| ave. | 2.842 | 2.841 | 2.840 | 2.843 |

*All standard errors are between 0.005 and 0.008 Å.

that the change in structure geometry over the temperature range 25 to 200°C appears negligible.

The invariance of structure geometry is further shown by two other sets of parameters. First, the values of O–T–O angles are practically constant. The maximum change over the four temperatures, for a given angle, is only 0.4°, and this is only twice one standard error. Secondly, the orientations of the principal axes of the thermal ellipsoids exhibit no regular changes as a function of temperature. They are essentially constant, within standard error, and therefore orientation values are listed in Table 6 only for the 25°C data.

Some regular changes are evident, however, in the interatomic distances, as shown in Tables 3 and 4. These distances have been calculated with no correction for thermal motion. The average T–O distances show a regular decrease for both Si(1) and

Si(2), with essentially no change for Al. The differences are small relative to the standard errors, but the consistency of change with increasing temperature indicates that the difference in behavior of Al–O and Si–O distances is real, particularly since equivalent trends are evident in average O–O distances of corresponding tetrahedra. Distances computed with corrections for thermal vibration all show a general increase with temperature. The actual trends in relative change of mean distances as a function of temperature cannot be calculated without a more exact model of atom interactions, because of thermal motion. Definite trends have appeared in some other crystal structures, however. In low cristobalite (Peacor, in preparation), and in low quartz (Young, 1962), average Si–O distances, as calculated without thermal corrections, show similar decreases with increasing temperature. In nepheline, however (Foreman and Peacor, 1970), the uncorrected distances show a decrease for Al–O and an increase in Si–O distances. Although the actual values of mean distances are in question, it is clear that different structures exhibit different trends in T–O distances as a function of temperature, and that Al–O and Si–O distances behave differently. The reasons are not yet apparent. The relatively

TABLE 5. T–O–T Angles*

| Atoms involved | 25°C | 88°C | 146°C | 198°C |
|---|---|---|---|---|
| Si(1)-O(1)-Al | 141.1° | 141.5° | 141.3° | 141.2° |
| Si(2)-O(2)-Al | 129.8 | 130.1 | 130.2 | 130.3 |
| Si(2)-O(3)-Al | 138.7 | 138.3 | 138.5 | 138.2 |
| Si(2)-O(4)-Al | 135.1 | 135.1 | 135.2 | 135.2 |
| Si(2)-O(5)-Si(1) | 144.4 | 144.6 | 144.9 | 144.8 |
| ave. | 137.8 | 137.9 | 138.0 | 137.9 |

*Standard errors are between 0.1 and 0.2°

TABLE 6. Magnitudes and Orientations of the Principal Axes of the Thermal Ellipsoids for Natrolite at 25°C

| Atom | Axis | Magnitude (Å) | Angle of axis to: a | b | c |
|---|---|---|---|---|---|
| Si(1) | 1 | 0.050(6) | 90 | 90 | 0 |
| | 2 | 0.088(2) | 65(7) | 154(7) | 90 |
| | 3 | 0.099(2) | 25(7) | 65(7) | 90 |
| Si(2) | 1 | 0.074(2) | 45(17) | 70(12) | 52(21) |
| | 2 | 0.079(2) | 122(26) | 107(35) | 38(21) |
| | 3 | 0.081(2) | 118(20) | 28(22) | 88(32) |
| Al | 1 | 0.067(2) | 87(4) | 6(13) | 85(14) |
| | 2 | 0.077(3) | 105(8) | 84(14) | 164(8) |
| | 3 | 0.091(2) | 15(7) | 92(3) | 105(8) |
| O(1) | 1 | 0.079(8) | 84(4) | 71(7) | 160(7) |
| | 2 | 0.117(4) | 105(5) | 155(6) | 110(7) |
| | 3 | 0.147(3) | 16(4) | 106(4) | 90(4) |
| O(2) | 1 | 0.083(4) | 27(13) | 63(12) | 86(26) |
| | 2 | 0.093(6) | 80(35) | 102(58) | 164(61) |
| | 3 | 0.097(4) | 115(16) | 30(29) | 105(63) |
| O(3) | 1 | 0.075(6) | 107(4) | 36(3) | 59(4) |
| | 2 | 0.118(3) | 162(4) | 100(6) | 105(6) |
| | 3 | 0.140(5) | 83(7) | 56(4) | 145(5) |
| O(4) | 1 | 0.076(5) | 37(3) | 116(4) | 66(3) |
| | 2 | 0.117(3) | 112(6) | 154(4) | 103(7) |
| | 3 | 0.139(5) | 62(4) | 88(7) | 152(5) |
| O(5) | 1 | 0.068(9) | 69(4) | 79(3) | 156(5) |
| | 2 | 0.122(4) | 150(5) | 107(6) | 114(5) |
| | 3 | 0.144(3) | 110(6) | 20(5) | 86(4) |
| Na | 1 | 0.115(2) | 56(4) | 48(5) | 61(5) |
| | 2 | 0.136(2) | 60(24) | 138(5) | 63(24) |
| | 3 | 0.139(3) | 48(21) | 90(22) | 138(21) |
| H₂O | 1 | 0.132(6) | 87(7) | 82(13) | 8(11) |
| | 2 | 0.149(3) | 70(6) | 159(8) | 84(13) |
| | 3 | 0.171(3) | 20(6) | 71(6) | 95(5) |

rapid increase in the magnitude of Na–O interatomic distances is consistent with similar changes for atoms other than Al and Si in a number of other structures.

Several authors, including Foreman and Peacor (1970) and Taylor (1972) have pointed out that thermal expansion should be a function of two variables: (1) increase in mean interatomic distances, and (2) changes in relative atom positions. The latter may be principally reflected in changes in $T–O–T$ angles (Table 5), and is a principal cause of significant thermal expansion in tektosilicates. The average $T–O–T$ angles in natrolite differ at 25 and 198°C by only 0.1°. This, as a consequence of the negligible shifts in coordinates, explains the lack of measurable change in the magnitudes of $a$ and $b$, as determined in an earlier part of this study.

The only structure parameters which differ between temperatures and from those of Meier (1960) are the equivalent isotropic temperature factors (Table 2). All changes are approximately linear relative to temperature, the changes being proportional to room temperature values; that is, those atoms having low temperature factors at room temperature, and thus high bonding force constants, show the smallest increases in temperature factor with increasing temperature. The order of increase as a function of atomic species is the same as found in some other tektosilicates, for example nepheline. The rapid increase in $B$ of $H_2O$, extrapolated to about 3.7 at 250°C, is an expression of the dehydration mechanism. Since the atomic positions are nearly invariant, the sizes of the channels through which $H_2O$ must diffuse also are unchanged. The dehydration is therefore brought about only through an increase in thermal energy of the $H_2O$ molecule, relative to the hydrogen bonds to O(1) and O(5).

## References

CRUICKSHANK, D. W. J. (1965) Errors in least squares methods. *In*, J. S. Rollett, Ed. *Computing Methods in Crystallography*. Pergamon Press, Oxford, p. 114.

FANG, J. H. (1963) Cell dimensions of dehydrated natrolite. *Amer. Mineral.* **48**, 414–417.

FOIT, F. F., AND D. R. PEACOR (1967) A high temperature furnace for a single crystal X-ray diffractometer. *J. Sci. Instrum.* **44**, 183–185.

FOREMAN, N., AND D. R. PEACOR (1970) Refinement of the nepheline structure at several temperatures. *Z. Kristallogr.* **132**, 45–70.

HEY, M. H., AND F. A. BANNISTER (1933) Studies on the zeolites. III. Natrolite and metanatrolite. *Mineral. Mag.* **23**, 243–289.

MEIER, W. M. (1960) The crystal structure of natrolite. *Z. Kristallogr.* **113**, 430–444.

PAULING, L. (1930) The structure of some sodium and calcium aluminosilicates. *Proc. Nat. Acad. Sci.* **16**, 453–459.

VAN REEUWIJK, L. P. (1972) High-temperature phases of zeolites of the natrolite group. *Am. Mineral.* **57**, 499–510.

TAYLOR, D. (1972) The thermal expansion behavior of the framework silicates. *Mineral. Mag.* **38**, 593–604.

TAYLOR, W. H., C. A. MEEK, AND W. W. JACKSON (1933) The structures of the fibrous zeolites. *Z. Kristallogr.* **84**, 373–398.

YOUNG, R. A. (1962) Mechanism of the phase transition in quartz. *Final report to Air Force Office of Scientific Research, Project* **A-447**.